

Amorphous concentrated spin-glasses: MnX ($X = Ge, C, Si-Te$)

J. J. Hauser

Bell Laboratories, Murray Hill, New Jersey 07974

(Received 17 March 1980)

Amorphous MnSi is a concentrated spin-glass. In order to understand the underlying reason, the following similar systems were investigated: Mn_3Ge_2 , MnGe, MnC, MnAs, and MnSb. In the case of MnAs and MnSb which are strong ferromagnets in the crystalline state, the amorphous films were ferromagnetic or superparamagnetic and no spin-glass transition could be detected. On the other hand, crystalline Mn_3Ge_2 is antiferromagnetic below 150 K and amorphous MnGe (*a*-MnGe) and *a*- Mn_3Ge_2 show spin-glass transitions at, respectively, 48 and 53 K. MnC does not exist as a stable crystalline compound. However, *a*-MnC films were obtained by sputtering at 77 K and such films show a definite spin-glass transition at 21 K. Metastable microcrystalline MnC films obtained by deposition at 400 K indicate that crystalline MnC is weakly magnetic below $T_C = 300$ K. This suggests that weak ferro- or ferrimagnetism or antiferromagnetism is required in the crystalline state in order to observe a spin-glass transition in the amorphous state. While MnX ($X = Si, Ge, C$) spin-glasses are metallic, a spin-glass transition has also been observed in semiconducting MnSi-MnTe mixtures.

I. INTRODUCTION

While crystalline MnSi is a weak ferromagnet with a 30-K Curie temperature (T_C), amorphous MnSi (*a*-MnSi) exhibits a spin-glass transition^{1,2} at 22 K. In order to understand the reason for this spin-glass transition, an empirical approach was chosen which consists in investigating similar systems. MnAs and MnSb were chosen because they are both strong ferromagnets in the crystalline state ($T_C = 318$ and 587 K, respectively). On the other hand, Mn_3Ge_2 is ferrimagnetic near 300 K and antiferromagnetic below 150 K (Refs. 3 and 4) while MnC does not exist as a stable crystalline compound. The closest composition studied is Mn_4C which has been reported to be ferrimagnetic⁵ or weakly magnetic.⁶ The main idea behind this study is to investigate whether some of these compounds show a spin-glass transition in the amorphous state and if so whether we can correlate the existence of the spin-glass transition with a particular magnetic interaction in the crystalline state.

Another aspect of the present study relates to the existence of a resistive anomaly at the spin-glass transition temperature (T_{SG}). It is well known that while spin-glasses display a sharp cusp in the susceptibility at T_{SG} , there is no anomaly in the resistivity. Indeed, it has been shown theoretically⁷⁻⁹ that in the vicinity of magnetic points, $d\rho(T)/dT$ varies as the magnetic specific heat. Since the magnetic specific heat shows no anomaly either, which is consistent with the predictions of the spin-glass theory,¹⁰ one would expect a smoothly varying resistivity. However, the temperature dependence of the resistivity has only been studied thus far in metals and the situation could be

quite different in an amorphous semiconductor. Since MnTe is a semiconductor¹¹ and *a*-MnSi a metallic spin-glass, alloys of MnSi and MnTe have been investigated with the hope of obtaining an amorphous semiconducting spin-glass.

II. EXPERIMENTAL PROCEDURE

All films were getter-sputtered onto sapphire wafers held at temperatures ranging from 77 to 370 K from the appropriate target. The various compounds investigated presented special metallurgical problems which were solved in different ways to obtain the sputtering target. Similarly to MnSi,^{1,2} the Mn_3Ge_2 and MnGe targets were obtained by melting inductively¹² in an alumina crucible under an argon atmosphere the required amount of high-purity Mn and Ge. The MnSb target was prepared¹³ in two different ways: (i) by melting in an evacuated quartz tube followed by quenching, and (ii) by hot pressing the powders at 400 °C for 6 h. Because of a transformation to Mn_2As occurring at higher temperatures, MnAs was obtained¹³ by cold pressing the powders and annealing in an evacuated quartz tube at 350 °C for 24 h. The MnTe compound was prepared¹³ by reacting the mixed powders at 800 °C in a graphite crucible which was inserted in an evacuated quartz tube. The various MnSi-MnTe alloys were obtained by mounting on a common stem pieces of MnSi and MnTe of various sizes. Since the compound MnC does not exist as a stable crystalline phase, the target was prepared by mixing and tumbling high-purity 325-mesh C and Mn powders followed by cold press-

ing in the form of a disk. Such a procedure has been shown¹⁴ to produce Ag-Ni films with a composition close to that of the nominal target composition. While x-ray fluorescence analysis was used to check the composition of Ag-Ni films, this was not possible with MnC films because of the low C scattering cross section. The composition of an MnC film was therefore obtained from the original weight gain and from the weight of the MnO film obtained by annealing this film in air for 10 min at 1000°C. Since the sputtering yield of MnC was very low, it was necessary to sputter at high power (60 W: 3000 V, 20 mA) and in order to keep the substrate temperature low, the sapphire substrate was cemented with Ga to the copper table through which liquid nitrogen was flowing. The film thickness was measured with a Sloane-Dektak step measuring apparatus. The amorphous nature of the films was ascertained by x-ray diffraction.

The ac susceptibility of the films was measured usually at 10 kHz with a modulating field of 4 Oe with a push rod susceptibility holder¹⁵ by warming up the sample in helium gas from 4.2 K to room temperature. The resistivity of the samples was obtained on a holder using four spring-loaded contacts.

III. EXPERIMENTAL RESULTS AND DISCUSSION

A. Metallic spin-glasses

Preliminary results on *a*-MnGe have been previously reported.¹⁶ The main result is that *a*-MnGe shows a spin-glass transition at $T_{SG} = 48$ K (Fig. 1). Similar to *a*-MnSi one finds that the film deposited at 77 K displays the smallest susceptibility peak (Fig. 1).

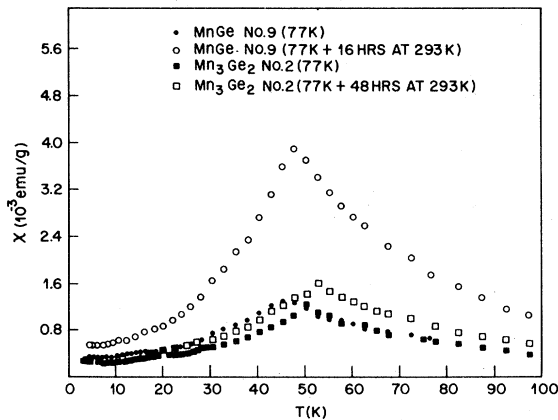


FIG. 1. Susceptibility vs temperature showing the spin-glass cusps at $T_{SG} \approx 48$ K for MnGe and at 53 K for Mn_3Ge_2 as a function of anneal.

The increased clustering with higher deposition temperature (T_D) results in an increase in both $\chi(T_{SG})$ and the ratio $R = \chi(T_{SG})/\chi(4.2 \text{ K})$. R increased from 2.2 to 4.3 for *a*-MnSi¹ and from 4.3 to 27 for *a*-MnGe as T_D increased from 77 K to 625 and 370 K, respectively. Furthermore, $\chi(T_{SG})$ reaches a maximum of 4.6×10^{-3} emu/g in *a*-MnSi and of 5.4×10^{-2} emu/g in *a*-MnGe. Since an increase in both χ and R was linked to increased clustering in the case of a *a*-MnSi,¹ the differences in χ and R between *a*-MnSi and *a*-MnGe would suggest a greater degree of clustering in *a*-MnGe. The reason for the greater clustering tendency in *a*-MnGe may come from the fact that MnSi is a stable crystalline phase while MnGe is not. Consequently, even in the amorphous state, MnGe will tend to phase separate into Mn_3Ge_2 (which is the closest known crystalline compound) and Ge. The validity of this idea can be tested by investigating *a*- Mn_3Ge_2 .

As shown in Fig. 1 *a*- Mn_3Ge_2 displays a spin-glass transition at $T_{SG} \approx 53$ K. The slightly higher T_{SG} for Mn_3Ge_2 than for MnGe is consistent with the slightly higher Mn content. It is clear from Fig. 1 that the clustering in Mn_3Ge_2 as revealed by the increase in $\chi(T_{SG})$ upon annealing is much smaller than in MnGe for similar annealing conditions. Furthermore, the maximum value for $\chi(T_{SG})$ obtained by deposition at 370 K is only 5.6×10^{-3} emu/g for Mn_3Ge_2 which is quite close to the value observed in *a*-MnSi (4.6×10^{-3} emu/g) and much smaller than that measured for *a*-MnGe (5.4×10^{-2} emu/g). One may therefore conclude that the tendency for phase separation increases clustering, and that minimal clustering upon annealing will be observed for amorphous compositions close to the stoichiometric compound.

The temperature dependence of the susceptibility for a 28- μ m-thick *a*-MnC film is shown in Fig. 2. The scatter in the data is more pronounced than for either *a*-MnSi or *a*-Mn-Ge owing to the fact that the specific susceptibility is an order of magnitude smaller. Nevertheless, the spin-glass transition at $T_{SG} = 21$ K is quite obvious in Fig. 2. Combining the film thickness with the weight-gain measurement results in a density of 4.9 g cm^{-3} for *a*-MnC. This is precisely the density one would obtain for an equiatomic mixture of Mn with density 7.43 g cm^{-3} and of *a*-C with density¹⁷ 1.9 g cm^{-3} which further supports the determination of the composition obtained from the MnC and MnO (obtained by annealing the film in air) weight measurements.

In order to find out the magnetic properties of crystalline MnC (which does not exist as a stable phase), MnC films were deposited at 400 K. Although, the diffraction patterns for such films are still amorphous, the appearance of magnetism as shown in Fig. 3 suggests that the films consist of metastable MnC microcrystals embedded in an *a*-MnC

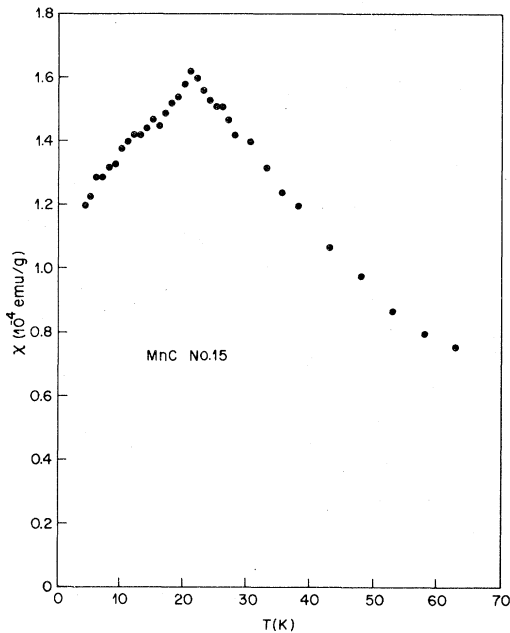


FIG. 2. Susceptibility vs temperature for a -MnC deposited at 90 K.

matrix. The actual specific magnetization of MnC could be quite larger than the very small value shown in Fig. 3 since the concentration of microcrystals in the film is unknown. The small value of the magnetization suggests weak ferrimagnetism or imperfect antiferromagnetism which as shown in Fig. 3 disap-

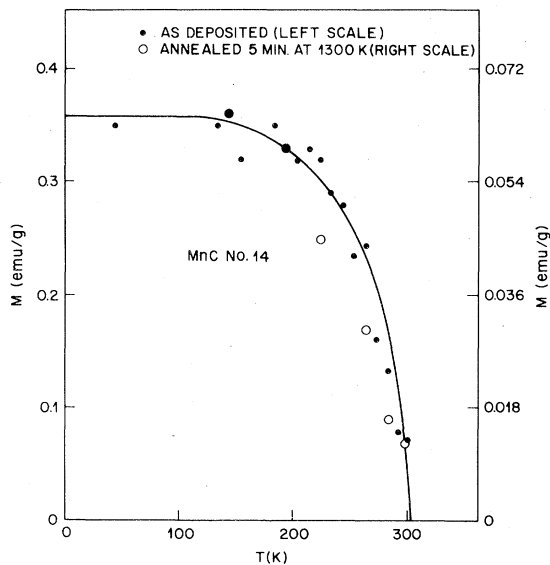


FIG. 3. Dependence of the magnetization on temperature for microcrystalline MnC deposited at 400 K and annealed at 1300 K.

pears at $T_C = 300$ K. The suggestion that the microcrystals are metastable MnC is further supported by the annealing experiment described in Fig. 3. This annealing treatment results in an 80% decrease of the magnetization and the resulting crystalline diffraction pattern consists of strong lines which correspond to Mn_3C_2 and of weaker lines which do not correspond to either Mn or any known Mn-C compounds (e.g., Mn_4C). It is reasonable to assume that these weak lines correspond to metastable crystalline MnC. Consequently, the as-deposited film which consists of metastable microcrystals of MnC in a -MnC phase separates upon annealing into the stable nonmagnetic Mn_3C_2 and free C. At any rate, it is clear from Fig. 3 that the crystalline counterpart to the a -MnC spin glass is only weakly magnetic.

Let us now turn our attention to MnSb and MnAs which are both strong ferromagnets in the crystalline state. Both materials had to be sputtered at 77 K to yield amorphous films. Amorphous MnSb films obtained from the solid and pressed powder targets had similar magnetic properties but dissimilar annealing behaviors. Films obtained from the pressed powder target remained amorphous at room temperature, while films sputtered from the solid target recrystallized somewhat below or at room temperature. The greater stability of the films deposited from the pressed powder target is undoubtedly produced by the inclusion in the film of the residual air trapped in the target. The main conclusion is that no spin-glass transition could be detected in either a -MnSb or a -MnAs. Indeed, a -MnSb films obtained from the solid target were ferromagnetic while a -MnSb and a -MnAs sputtered from pressed powder targets are superparamagnetic as shown in Fig. 4 for an a -MnSb film.

It is therefore clear that amorphous films obtained from a material with a strong ferromagnetic interaction (MnAs and MnSb) do not show a spin-glass transition. On the other hand the amorphous spin-

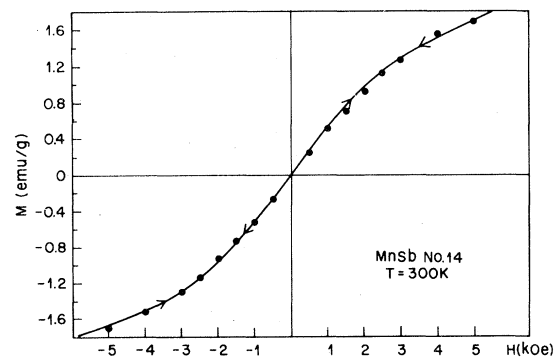


FIG. 4. Reversible magnetization for a superparamagnetic a -MnSb film sputtered from a pressed-powder target.

glasses (*a*-MnSi, *a*-Mn-Ge, and *a*-MnC) have a corresponding crystalline phase which is either weakly ferromagnetic (ferrimagnetic) or antiferromagnetic. In other words, the material most likely to produce a spin-glass behavior in the amorphous state is one in which the spin interactions in the crystalline state are neither strongly ferromagnetic nor strongly antiferromagnetic. In this case, the disorder induced by the amorphous state can easily result in random interactions of both types (ferromagnetic and antiferromagnetic), i.e., in a spin-glass.

B. Semiconducting spin-glass (*a*-Mn-Si-Te)

As mentioned above, the electrical resistivity of metallic spin-glasses varies smoothly through T_{SG} which is consistent with the prediction of the spin-glass theory. The situation could be different in an amorphous semiconducting spin-glass. Indeed, if one could obtain an amorphous semiconductor with variable range hopping, i.e., where the resistivity (ρ) can be fitted to the relation

$$\rho = \rho_0 \exp(T_0/T)^{1/4} \quad (1)$$

and $T_0 = 16\alpha^3/kN(E_F)$ where α^{-1} is the width of the localized state wave functions and $N(E_F)$ the density of localized states at the Fermi level (E_F) one may expect an anomaly in ρ at T_{SG} for the following reason. At low temperatures, the optimum energy spacing W between energy states near E_F is given by¹⁸

$$(W_{opt})^{4/3} = \left[\frac{3(2\alpha)^3}{4\pi N(E_F)} \right]^{1/3} \frac{kT}{3} \quad (2)$$

Since the magnetic energy involved with the spin-glass transition is of order kT_{SG} one would expect from relation (2) a strong coupling between the spin-glass transition and the hopping energy W and therefore some anomaly in the resistivity ρ .

A likely candidate for this study is MnTe which is known to be an antiferromagnetic semiconductor.¹¹ Amorphous films of MnTe could only be obtained by sputtering at 77 K but remained amorphous upon warming up to room temperature. As shown in Fig. 5 it is clear that the resistivity of *a*-MnTe satisfies relation (1). The slight deviations to higher slopes below 28 K in the as-deposited film and below 58 K in the annealed film occur in all *a*-MnTe films and are not fully understood. They may be caused by a different defect state which prevails at low temperatures. The increase in the value of T_0 after annealing corresponds to a decrease in $N(E_F)$ as a result of the removal of defect states introduced by the low deposition temperature. Similar effects have been reported for other amorphous semiconductors such as *a*-Ge (Ref. 19) and *a*-Si (Ref. 20) deposited at 77 K. The value of T_0 for the annealed sample corresponds to

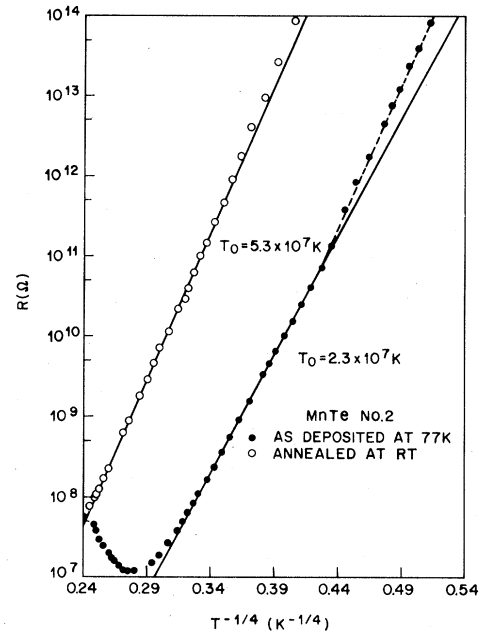


FIG. 5. Temperature dependence of the resistance for *a*-MnTe deposited at 77 K ($\rho_{300K} = 1.25 \times 10^3 \Omega \text{cm}$).

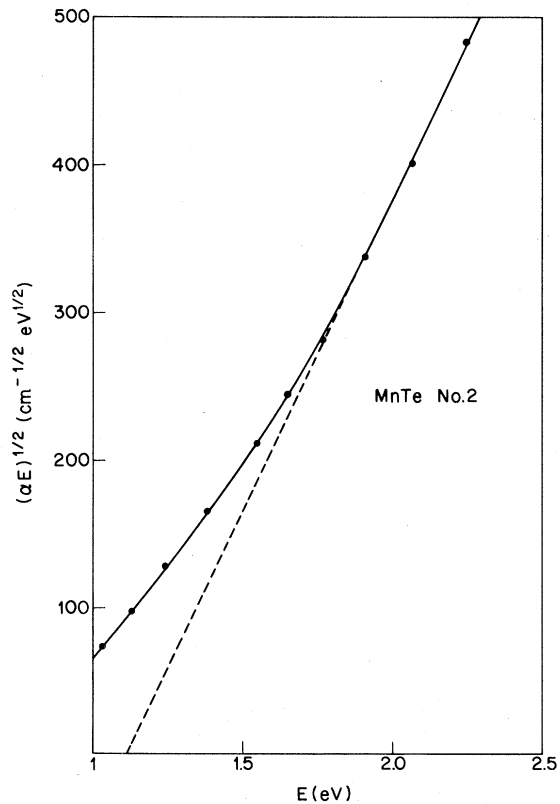


FIG. 6. Plot of $(\alpha E)^{1/2}$ where α is the optical absorption vs the photon energy E .

$N(E_F) \approx 3.5 \times 10^{18}$ states $\text{eV}^{-1} \text{cm}^{-3}$ (for a typical α^{-1} value of 10 \AA) which is also very close to the values obtained on $a\text{-Ge}$ (Ref. 19) and $a\text{-Si}$.²⁰ The optical gap of $a\text{-MnTe}$ as obtained²¹ from the extrapolation to zero absorption in Fig. 6 is 1.1 eV which is very close to the 1.3-eV value reported¹¹ for crystalline MnTe. Unfortunately, although $a\text{-MnTe}$ has the prerequisite semiconducting properties for the present study it does not display a spin-glass transition: the low-temperature susceptibility is essentially temperature independent and equal to $(7 \pm 1) \times 10^{-5}$ emu/g. The absence of a spin-glass transition in $a\text{-MnTe}$ is however consistent with the discussion in Sec. I of this paper based on the fact that crystalline MnTe is a strong antiferromagnet with the highest Néel temperature (323 K) of the manganese chalcogenides.¹¹

The solution to this impasse should reside in alloying $a\text{-MnTe}$ (the proper amorphous semiconductor) with the spin-glass $a\text{-MnSi}$. Since the various MnTe-MnSi alloys were obtained by sputtering from a composite target consisting of pieces of MnSi and MnTe of varying sizes, the absolute composition of the film was determined using atomic absorption²² for only one film with a composition close to the threshold of spin-glass behavior. The absolute composition is not crucial to the present study since one is mainly interested in linking the susceptibility and the resistivity behaviors for a given semiconducting composition irrespective of its actual composition. The relative composition of the MnTe-MnSi films was checked in two different ways. As one adds more MnSi one observes with x-ray-fluorescence analysis the monotonic increase of Si counts and the decrease in Te counts. Furthermore, both the resistivity and T_0 decrease with increasing MnSi content. This decrease in T_0 which results from an increase in $N(E_F)$ has been observed in several other amorphous semiconductors doped with metallic impurities.^{23,24} The addition of MnSi to MnTe has also the advantage of stabilizing the amorphous phase: while $a\text{-MnTe}$ films could only be obtained with $T_D = 77 \text{ K}$, $a\text{-MnTe-MnSi}$ films can be deposited at $T_D = 300 \text{ K}$.

The $a\text{-MnTe-MnSi}$ films can be divided in two categories depending on the MnSi concentration. Films containing less than about 50 mole % MnSi are MnTe-like, i.e. they show no spin-glass behavior, $\rho(300 \text{ K}) \geq 1 \text{ } \Omega \text{ cm}$ and the exponent T_0 in relation (1) is $\geq 1.2 \times 10^6 \text{ K}$ which corresponds to $N(E_F) \leq 1.5 \times 10^{20}$ states $\text{eV}^{-1} \text{cm}^{-3}$. On the other hand, films with $\rho(300 \text{ K}) < 1 \text{ } \Omega \text{ cm}$ which contain more than 50 mole % MnSi display a spin-glass transition as shown in Fig. 7. The composition of MnTe-MnSi No. 2 is 65 mole % MnSi as obtained by atomic absorption spectroscopy. The temperature dependence of the resistance for films of similar compositions to those displaying a susceptibility cusp in Fig. 7 is shown in Fig. 8.

Before discussing whether a resistive anomaly can

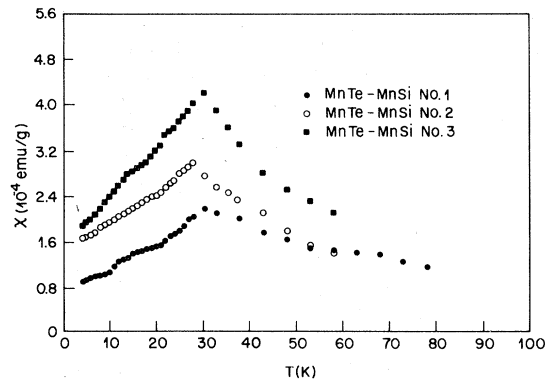


FIG. 7. Susceptibility vs temperature showing the spin-glass cusps for MnTe-MnSi films of various compositions.

be identified with T_{SG} , it is useful to point out the difficulties associated with such an experiment. As mentioned above, the conductivity of the films must be in the hopping regime. However, even MnTe-MnSi No. 3 which contains an appreciable amount of MnTe is already out of the hopping regime as shown by the continuously downward bending curve (Fig. 8). The departure from variable

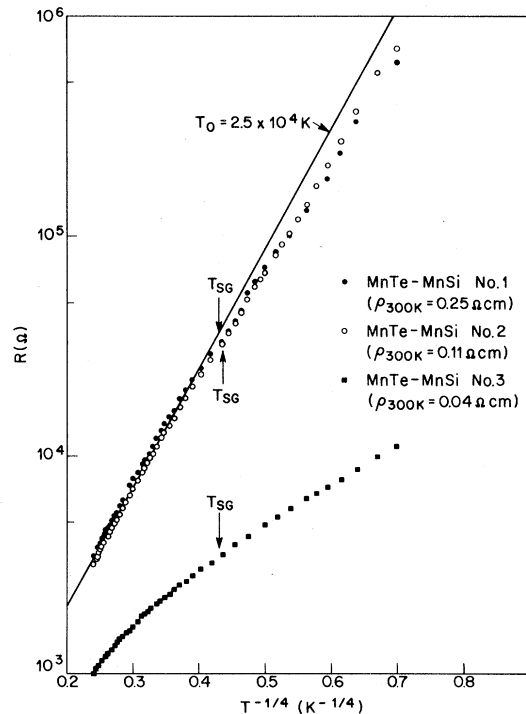


FIG. 8. Temperature dependence of the resistance for MnTe-MnSi films with similar compositions to those displaying a susceptibility cusp in Fig. 7. The arrows marked T_{SG} correspond to the temperatures of the susceptibility maxima shown in Fig. 7.

range hopping in such a film is due to the fact that $N(E_F)$ has exceeded the delocalization limit of $\simeq \alpha^3 = 10^{21}$ states $\text{cm}^{-3} \text{eV}^{-1}$. The large amount of MnTe in this film is clearly revealed by the following three factors: the susceptibility at T_{SG} (Fig. 7) is about an order of magnitude smaller than that of pure α -MnSi (Refs. 1 and 2); the room-temperature resistivity ($0.04 \Omega\text{cm}$) and the increase of R with decreasing T are both an order of magnitude larger than those for α -MnSi. Nevertheless, the resistance curve shown in Fig. 8 displays a smooth dependence on temperature with no anomaly at T_{SG} which was expected from the fact that the conductivity states are delocalized in MnTe-MnSi No. 3.

On the other end of the spectrum where clear variable range hopping can be observed [$N(E_F) \leq 1.5 \times 10^{20}$ states $\text{eV}^{-1} \text{cm}^{-3}$], there is not enough MnSi to cause the spin-glass transition. Consequently, the hopping conductivity and the spin-glass transition can only coexist over a very narrow range of compositions. But unfortunately, in this range of compositions, $N(E_F) > 1.5 \times 10^{20}$ states $\text{eV}^{-1} \text{cm}^{-3}$ and is therefore close to the delocalization limit and one expects deviations from relation (1).

The best evidence for a resistive anomaly is given in Fig. 8 for MnTe-MnSi No. 1 and No. 2. Because

of the low value of T_0 which corresponds to $N(E_F) = 7 \times 10^{21}$ states $\text{eV}^{-1} \text{cm}^{-3}$ one expects some downward deviations from a straight line at low temperatures. However, while the data for MnTe-MnSi No. 3 can be fitted by a smooth curve, an attempt to do the same for MnTe-MnSi No. 1 and No. 2 leaves an inflection point in the vicinity of T_{SG} (the curve was not drawn in order not to bias the reader). The data for MnTe-MnSi No. 1 and No. 2 are best fitted by a straight line with slope $T_0 = 2.5 \times 10^4$ K above T_{SG} and another straight line with half that slope below T_{SG} . In conclusion, although a resistive anomaly has not been clearly established, the data presented here are the first for an amorphous semiconducting spin-glass and linked with theoretical expectations suggest that a resistive anomaly at T_{SG} may indeed exist.

ACKNOWLEDGMENTS

I would like to thank S. Greenberg-Kosinski for suggesting the measurement of Mn_3Ge_2 and for her able technical assistance. I would also like to acknowledge the technical assistance of J. E. Bernardini, L. D. Blitzer, V. G. Lambrecht, Jr., and G. A. Pasteur.

- 1J. J. Hauser, *Solid State Commun.* **30**, 201 (1979).
- 2J. J. Hauser, F. S. L. Hsu, G. W. Kammlott, and J. V. Waszczak, *Phys. Rev. B* **20**, 3391 (1979).
- 3L. G. Fakidov and Y. N. Tsiovkin, *Fiz. Met. Metalloved.* **7**, 685 (1959) [*Phys. Metals Metallog. (USSR)* **7**, 47 (1959)].
- 4J. S. Kouvel, in *Intermetallic Compounds*, edited by J. H. Westbrook (Wiley, New York, (1967), p. 553.
- 5K. Knox, Annual Meeting ACA, Ithaca, July 1959 (unpublished).
- 6R. M. Bozorth, *Ferromagnetism* (Van Nostrand, Princeton, New Jersey, 1961), p. 337.
- 7M. E. Fisher and J. S. Langer, *Phys. Rev. Lett.* **20**, 665 (1968).
- 8T. G. Richard and D. J. W. Geldart, *Phys. Rev. Lett.* **30**, 290 (1973).
- 9T. G. Richard and D. J. W. Geldart, *Phys. Rev. B* **15**, 1502 (1977).
- 10P. W. Anderson, *J. Appl. Phys.* **49**, 1599 (1978); and in *Lectures on Amorphous Systems, Summer School at Les Houches, France, 1979*, edited by R. Balian (North-Holland, Amsterdam, 1979), p. 162.
- 11J. W. Allen, G. Lucovsky, and J. C. Mikkelsen, Jr., *Solid State Commun.* **24**, 367 (1977), and reference therein.
- 12I am indebted to J. E. Bernardini for the preparation of these targets.
- 13I am indebted to V. G. Lambrecht, Jr., for the preparation of these targets.
- 14J. J. Hauser, *Phys. Rev. B* **12**, 5160 (1975).
- 15J. J. Hauser and C. M. Antosh, *Rev. Sci. Instrum.* **47**, 156 (1976).
- 16J. J. Hauser, in *Proceedings of the International Conference on Magnetism, Munich, 1979*, edited by W. Zinn, G. M. Kalvius, and E. Feldtkeller (North-Holland, Amsterdam, 1980), p. 1387.
- 17J. J. Hauser, *J. Non-Cryst. Solids* **23**, 21 (1977).
- 18N. F. Mott and E. A. Davis, *Electronic Processes in Non-Crystalline Materials* (Clarendon, Oxford, England, 1979), p. 34.
- 19J. J. Hauser and A. Staudinger, *Phys. Rev. B* **8**, 607 (1973).
- 20J. J. Hauser, *Phys. Rev. B* **8**, 3817 (1973).
- 21I am indebted to G. A. Pasteur for performing the infrared optical-absorption measurements.
- 22I am indebted to L. D. Blitzer for the atomic absorption analysis.
- 23J. J. Hauser, *Solid State Commun.* **13**, 1451 (1973).
- 24J. J. Hauser, *Phys. Rev. B* **9**, 2544 (1974).